ASK1 inhibitor NQDI-1 decreases oxidative stress and neuroapoptosis via the ASK1/p38 and JNK signaling pathway in early brain injury after subarachnoid hemorrhage in rats

JIAJIA DUAN[1], WEN YUAN[2], JUAN JIANG[3], JIKAI WANG[4], XIAOXIN YAN[3], FEI LIU[4] and AIHUA LIU[1,5]

[1]Department of Neurosurgery, Third Xiangya Hospital, Central South University, Changsha, Hunan 410000; [2]Department of Neurosurgery, Zhuzhou Central Hospital, Zhuzhou, Hunan 412000; [3]Department of Anatomy and Neurobiology, Xiangya Medicine School, Central South University, Changsha, Hunan 410000; [4]Department of Neurosurgery, The Fifth Sun Yet-sen Hospital, Sun Yet-sen University, Zhuhai, Guangdong 519000; [5]Beijing Neurosurgical Institute, Beijing Tiantan Hospital, Capital Medical University, Beijing 100070, P.R. China

Received August 13, 2022; Accepted November 30, 2022

DOI: 10.3892/mmr.2023.12934

Abstract. Oxidative stress and neuroapoptosis are key pathological processes after subarachnoid hemorrhage (SAH). The present study evaluated the anti-oxidation and anti-apoptotic neuroprotective effects of the apoptosis signal-regulating kinase 1 (ASK1) inhibitor ethyl-2,7-dioxo-2,7-dihydro-3H-naphtho(1,2,3-de) quinoline1-carboxylate (NQDI-1) in early brain injury (EBI) following SAH in a rat model. A total of 191 rats were used and the SAH model was induced using monofilament perforation. Western blotting was subsequently used to detect the endogenous expression levels of proteins. Immunofluorescence was then used to confirm the nerve cellular localization of ASK1. Short-term neurological function was assessed using the modified Garcia scores and the beam balance test 24 h after SAH, whereas long-term neurological function was assessed using the rotarod test and the Morris water maze test. Apoptosis of neurons was assessed by TUNEL staining and oxidative stress was assessed by dihydroethidium staining 24 h after SAH. The protein expression levels of phosphorylated (p-)ASK1 and ASK1 rose following SAH. NQDI-1 was intracerebroventricularly injected 1 h after SAH and demonstrated significant improvements in both short and long-term neurological function and significantly reduced oxidative stress and neuronal apoptosis. Injection of NQDI-1 caused a significant decrease in protein expression levels of p-ASK1, p-p38, p-JNK, 4 hydroxynonenal, and Bax and significantly increased the protein expression levels of heme oxygenase 1 and Bcl-2. The use of the p38 inhibitor BMS-582949 or the JNK inhibitor SP600125 led to significant decreases in the protein expression levels of p-p38 or p-JNK, respectively, and a significant reduction in oxidative stress and neuronal apoptosis; however, these inhibitors did not demonstrate an effect on p-ASK1 or ASK1 protein expression levels. In conclusion, treatment with NQDI-1 improved neurological function and decreased oxidative stress and neuronal apoptosis in EBI following SAH in rats, possibly via inhibition of ASK1 phosphorylation and the ASK1/p38 and JNK signaling pathway. NQDI-1 may be considered a potential agent for the treatment of patients with SAH.

Correspondence to: Professor Fei Liu, Department of Neurosurgery, The Fifth Sun Yet-sen Hospital, Sun Yet-sen University, 52 Meihuadong Road, Xiangzhou, Zhuhai, Guangdong 519000, P.R. China
E-mail: doctorlf@126.com

Professor Aihua Liu, Beijing Neurosurgical Institute, Department of Interventional Neuroradiology, Beijing Tiantan Hospital, Capital Medical University, 119 South Fourth Ring West Road, Fengtai, Beijing 100070, P.R. China
E-mail: liuaihuadoctor@163.com

Key words: subarachnoid hemorrhage, NQDI-1, apoptosis signal-regulating kinase 1, oxidative stress, apoptosis, early brain injury

Introduction

Subarachnoid hemorrhage (SAH) is a serious acute cerebrovascular disease caused by the flow of blood into the subarachnoid space of the brain (1). However, at present, there are no effective drugs available for improving brain tissue damage after SAH following the prevention of rebleeding (2). Therefore, further studies into the mechanisms of brain injury following SAH and the exploration of appropriate treatment options for the improvement of the prognosis of SAH are urgently required.

Early brain injury (EBI) refers to secondary brain tissue damage caused by multiple physiological disturbances and a range of pathological changes that occur within 72 h of the onset of SAH (3). In the acute response phase following SAH, the injury begins with the entry of large amounts of blood into the subarachnoid space and this is followed by a series of pathological injuries (4). As mitochondria are particularly susceptible to hypoxia and ischemic injury, mitochondrial

dysfunction is one of the primary pathological injuries suffered after SAH (5). Large numbers of reactive oxygen species (ROS) are released, which leads to enhancement of oxidative stress and activation of the mitochondrial apoptotic pathway, causing mitochondrial injury and dysfunction (6). Therefore, therapeutic modalities that reduce oxidative stress and apoptosis are key for the improvement of the prognosis of SAH.

Apoptosis signal-regulating kinase 1 (ASK1), a member of the mitogen-activated protein 3 kinase (MAP3K) family, is activated by numerous different types of cellular stress and has an important role in oxidative stress and apoptosis (7). In primary cultures of mouse hippocampal neurons, the Rho kinase inhibitor fasudil reverses β-amyloid-induced elevation of phosphorylated (p-)ASK1, which decreases neuronal apoptosis in Alzheimer's disease (8). To the best of our knowledge, however, therapeutic options targeting ASK1 following SAH have not been evaluated.

Ethyl-2,7-dioxo-2,7-dihydro-3H-naphtho(1,2,3-de)quinoline-1-carboxylate (NQDI-1) has been reported to be a specific inhibitor of ASK1 and has been validated using *in vitro* kinase assays (9,10). Previous studies have reported that NQDI-1 may be effective in the treatment of numerous diseases through inhibition of ASK1 activity (11,12). NQDI-1 alleviates microcystin-LR-induced mitochondrial damage and apoptosis in ovarian granulosa cells via inhibition of the activation of ASK1 (13). Furthermore, indomethacin can induce apoptotic cascade responses in glial cells via ASK1 activation of endoplasmic reticulum stress (14). Therefore, the ASK1-specific inhibitor NQDI-1 may exert neuroprotective effects following SAH through inhibition of ASK1 activity. p38 and JNK are considered to form the downstream signaling pathways of ASK1; activated p38 and JNK are able to further activate a variety of substrates, including nuclear transcription factors as well as protein kinases and other functional proteins, which leads to the onset of oxidative stress and apoptosis (15).

It was hypothesized that ASK1 inhibitor NQDI-1 exerts neuroprotective effects and decreases oxidative stress and neuroapoptosis via the ASK1/p38 and JNK signaling pathway in EBI following SAH in rats.

Materials and methods

Experimental animals. The animal experiments were approved by the Ethics Committee for Experimental Animals of Central South University (approval no. 2019sydw0104). A total of 191 male Sprague-Dawley (SD) rats weighing 280-320 g were housed in a constant temperature (21-23˚C) and humidity (45-50%) environment with a 12/12-h light/dark cycle and had free access to water and food. All animal experiments were performed according to the Animal Research: Reporting *In Vivo* Experiments guidelines (16) and were performed in accordance with the National Institutes of Health (NIH) Guide for the Care and Use of Animals guidelines (17). When rats reached the designated preset time point of the experiment or met certain criteria for euthanasia [complete loss of appetite for 24 h or poor appetite (50% below normal) for 3 days, inability to eat or drink, or they were assessed as being close to death (self-injurious behavior, abnormal posture, respiratory distress, etc.)], the rats were placed in a carbon dioxide euthanasia device with CO_2 volume displacement rate set at 30%/min (18). Death was confirmed by cessation of breathing and heartbeat and pupil dilation. The carcasses of all rats were bagged and frozen for environmentally sound disposal.

SAH model. The rat SAH model was induced using monofilament perforation (19). After anesthetizing the rats (induction, 3% isoflurane; maintenance, 2% isoflurane), the left common, internal and external carotid artery of the rats were exposed. The distal external carotid artery was clipped using cauterization to form the stump of the external carotid artery. A 3-cm sharpened model 4-0 prolene wire was inserted ~2 cm through the external carotid artery until a slight resistance was felt. The puncture line was slowly advanced by ~3 mm to puncture the arterial wall. Brain tissue was removed at the corresponding time points predetermined for the experiment. If a blood clot was found on the ventral side of the brain tissue, it indicated that the rat had SAH. Rats with a score >8 by assessment of the SAH grading score were considered to meet the experimental requirements and to be a successful model. The procedure for the sham group was similar to that of the SAH group, with the exception that the 4-0 prolene wire did not pierce the arterial wall. The respiration, heart rate, skin color and pedal reflex were monitored every 5 min throughout the surgical and anesthetic recovery stages. Of these, 23 rats died and 8 rats were excluded, and these deaths and exclusions were supplemented by new SAH modeled rats.

Severity of SAH. The severity of SAH was assessed using SAH grading score 24 h after SAH (20). The ventral side of the brain tissue was divided into 6 regions, each rated 0-3 depending on the amount of blood clot and how well the blood vessels were obscured: A score of 0 indicates no clot, 1 indicates a small amount of clot, 2 indicates a moderate amount of clot but large vessels at the skull base are still identifiable, and 3 indicates a large amount of clot and unidentifiable vessels at the skull base. The six regional scores were summed to calculate a total score (0-18), where higher scores indicated more severe hemorrhage. Rats with a total SAH grade score of ≤8 were considered to have mild SAH, excluded from subsequent experiments and were replaced with newly modeled rats.

Drug administration. To enable the drug concentrations in the brain tissue to be more precisely regulated independently of the liver and other factors, the siRNAs and NQDI-1 were administered by intracerebroventricularly injection (21). Following anesthetization (induction, 3% isoflurane; maintenance, 2% isoflurane), the rats were fixed on a brain stereotaxic apparatus. The microinjector was fixed to the bregma at 1.0 posterior, 1.5 right and 3.3 mm deep. The ASK1 siRNA (cat. no. 4390771; Thermo Fisher Scientific, Inc.) or Scr siRNA control (cat. no. 4390843; Thermo Fisher Scientific, Inc.) were dissolved in 5 μl nuclease-free sterile deionized water at a concentration of 500 pmol and administered 48 h before SAH. The sequences of ASK1 siRNA were as follows: Sense 5'-CGG CAGACAUUGUUAUCAAtt-3' and antisense 5'-UUGAUA ACAAUGUCUGCCGtc-3'. Drug concentrations and doses reported in a similar study (22) and the solubility of NQDI-1 were used to determine the concentrations used in the present study. Three doses of NQDI-1 (1, 3 and 10 μg/kg; Selleck Chemicals) or vehicle solution in a total volume of 5 μl/rat

was injected 1 h after SAH. The BMS-582949 (100 mg/kg; Selleck Chemicals), SP600125 (30 mg/kg; Selleck Chemicals) and vehicle solutions could cross the blood-brain barrier and were administered intraperitoneally 1 h after SAH (23,24).

Short-term neurological function. Modified Garcia score and the beam balance score were used to assess the short-term neurological function 24 h after SAH. The modified Garcia score was divided into six categories as follows: Voluntary movement, voluntary limb movement, forepaw extension, climbing ability, somatosensory responses and tentacle response, each of which was scored individually and summed to give a total score ranging from 3-18 (25). Higher scores were considered to indicate better neurological function. For the beam balance score, rats were placed on a beam for 1 min and a score ranging from 0-4 was assessed based on the distance walked (26). Higher scores were considered to indicate better neurological function.

Long-term neurological function. Rotarod pre-adaptation experiments were performed on rats using the same initial velocity and acceleration before SAH modeling. The rats were placed on a Rotamex rotating bar tester (Columbus Instruments) for the Rotarod test on days 7, 14 and 21 after SAH (27). First, the initial Rotarod speed was set to 5 revolutions per min and the acceleration to 2 revolutions per 5 sec. After putting on the rats, the fall latency of the rats was recorded. The rats were then allowed to rest for 1 h. Finally, the fall latency of the rats was tested again at the initial speed of 5 revolutions per min and an acceleration of 2 revolutions per 5 sec. Longer fall latency was considered to indicate better motor coordination of the rat. At week 4 after SAH modeling, the Morris water maze test was used to assess learning memory and spatial orientation of the rats (27). The learning exercise of swimming and finding a platform located below the water surface was performed from day 1 to day 5 on week 4 (days 28-33 post-SAH) and the swimming trajectory, escape latency and swimming distance were recorded. On the final day, the platform was removed for testing and swimming trajectory, swimming distance and probe quadrant duration were recorded for 60 sec.

IF staining. After sequential perfusion of 4˚C saline and 4˚C 4% paraformaldehyde from the heart to remove blood from the brain tissue, intact brain tissue was obtained. After sucrose gradient dehydration, the brain tissue was then cut into 10-μm sections in a coronal position and was stored at -20˚C. IF staining was used to assess the co-localization of ASK1 with nerve cells. Frozen tissue sections were blocked using 5% donkey serum (cat. no. G1217-5ML; Wuhan Servicebio Technology Co., Ltd.) for 2 h at room temperature and incubated overnight at 4˚C with primary antibodies as follows: Anti-ASK1 (mouse; 1:200; cat. no. 67072-1-Ig; ProteinTech Group, Inc.), anti-NeuN (rabbit; 1:200; cat. no. 26975-1-AP; ProteinTech Group, Inc.), anti-ionized calcium-binding adapter molecule-1 (Iba-1; rabbit; 1:200; cat. no. 10904-1-AP; ProteinTech Group, Inc.), and anti-glial fibrillary acidic protein (GFAP; chicken; 1:200; cat. no. ab4674; Abcam). The tissue sections were then incubated for 2 h at room temperature with the corresponding fluorescent secondary antibodies as follows: Alexa Fluor® 594 AffiniPure Donkey Anti-Mouse IgG (H+L) (cat. no. 715-585-150; 1:500; Jackson ImmunoResearch Laboratories, Inc.), Alexa Fluor 488 AffiniPure Donkey Anti-Rabbit IgG (H+L) (cat. no. 711-545-152; 1:500; Jackson ImmunoResearch Laboratories, Inc.), and Alexa Fluor 488 AffiniPure Donkey Anti-Chicken IgY (IgG) (H+L) (cat. no. 703-545-155; 1:500; Jackson ImmunoResearch Laboratories, Inc.). Subsequently, they were stained for cell nuclei using 2 μg/ml DAPI (cat. no. G1012-100ML; Wuhan Servicebio Technology Co., Ltd.) for 10 min at room temperature. The sections were assessed using an Olympus BX53 fluorescence microscope (Olympus Corporation) and images were captured.

Dihydroethidium (DHE) staining. DHE staining was performed to assess the brain oxidative stress (28). Frozen brain tissue sections were incubated with 2 μmol/l DHE (Thermo Fisher Scientific, Inc.) at 37˚C for 30 min in the dark. After staining for cell nuclei using 2 μg/ml DAPI for 10 min at room temperature, the sections were assessed using an Olympus BX53 fluorescence microscope. A total of six sections from each brain tissue was randomly selected and six areas in each section were randomly selected for imaging. The number of DHE-positive cells was counted using ImageJ 1.4 software (National Institutes of Health) and the mean was calculated and taken as the final percentages for each brain tissue section.

TUNEL staining. TUNEL staining was used to evaluate the percentage of apoptotic neurons (29). Frozen tissue sections were blocked using 5% donkey serum for 2 h at room temperature and incubated overnight at 4˚C with primary antibody anti-NeuN (rabbit; 1:200; cat. no. 26975-1-AP; ProteinTech Group, Inc.). The tissue sections were then incubated with the fluorescent secondary antibody Alexa Fluor 488 AffiniPure Donkey Anti-Rabbit IgG (H+L) (cat. no. 711-545-152; 1:500; Jackson ImmunoResearch Laboratories, Inc.) for 2 h at room temperature. TUNEL staining was performed using the One Step TUNEL Apoptosis Assay kit (cat. no. C1090; Beyotime Institute of Biotechnology) according to the manufacturer's protocol. Finally, the tissue sections were stained for cell nuclei using 2 μg/ml DAPI for 10 min at room temperature. Random selection of TUNEL counting locations and calculation of TUNEL-positive neurons for each section were performed using the aforementioned method for DHE counting.

Western blotting (WB). WB was used to semi-quantify protein expression levels. After perfusion of 4˚C saline from the heart to remove blood from the brain tissue, intact brain tissue was obtained. Previous studies have reported that the SAH model, induced via left-sided endovascular puncture, results in a degree of bias towards bleeding events and can be relatively severe in terms of damage to left-sided brain tissue (30). Therefore, the left-sided brain tissue was used to assess the pathological damage following SAH modeling. Brain tissue proteins were extracted using RIPA lysis solution (cat. no. P0013B; Beyotime Institute of Biotechnology) according to the manufacturer's protocol. The protein concentration of the samples was determined by the BCA assay (cat. no. P0012; Beyotime Institute of Biotechnology) and subsequently adjusted to 5 μg/μl by adding different amounts of double-distilled water. The 5 μl

of 5 μg/μl protein samples were added to each lane and these protein samples were separated on 10% gels by SDS-PAGE electrophoresis and transferred to PVDF membranes. The membranes were blocked for 2 h at room temperature using 5% non-fat powdered milk (cat. no. P0216-300g; Beyotime Institute of Biotechnology). The membranes were incubated overnight at 4˚C with primary antibodies as follows: Anti-p-ASK1 (Ser-83; 1:1,000; cat. no. MA5-28020; Thermo Fisher Scientific, Inc.), anti-ASK1 (1:1,000; cat. no. 8662; Cell Signaling Technology, Inc.), anti-p-p38 MAPK (Thr180/Tyr182) (1:1,000; cat. no. 9216; Cell Signaling Technology, Inc.), anti-p38 MAPK (1:1,000; cat. no. 8690; Cell Signaling Technology, Inc.), anti-phospho-stress-activated protein kinase/Jun-amino-terminal kinase (phospho-SAPK/JNK) (Thr183/Tyr185; 1,000; cat. no. 9255; Cell Signaling Technology, Inc.), anti-SAPK/JNK (JNK; 1:1,000; cat. no. 9252; Cell Signaling Technology, Inc.), anti-4 hydroxynonenal (4-HNE; 1:1,000; cat. no. ab46545; Abcam), anti-heme oxygenase 1 (HO-1; 1:1,000; cat. no. 82206; Cell Signaling Technology, Inc.), anti-Bcl-2 (1:1,000; cat. no. 26593-1-AP; ProteinTech Group, Inc.), anti-Bax (1,1000; cat. no. 60267-1-Ig; ProteinTech Group, Inc.) and anti-β-actin (1:2,000; cat. no. 4970; Cell Signaling Technology, Inc.). This was followed by incubation with the appropriate horseradish peroxidase-conjugated secondary antibodies for 2 h at room temperature: Goat anti-mouse IgG-HRP (cat. no. sc-2005; 1:5,000; Santa Cruz Biotechnology, Inc.) or goat anti-rabbit IgG-HRP (cat. no. sc-2004; 1:5,000; Santa Cruz Biotechnology, Inc.), and the specific bands were visualized using an ECL kit (cat. no. P0018AS; Beyotime Institute of Biotechnology) and imaged using a UVP Che Studio PLUS system (Analytik Jena GmbH). Relative densitometric analysis of WB bands was performed using ImageJ 1.4 software (NIH) and the protein expression levels were normalized against β-actin.

Experimental design

Expression changes and cellular localization of ASK1 following SAH. A total of 36 rats were randomly assigned to six groups (n=6/group) as follows: i) Sham-operated (sham), ii) 3 h post-SAH, iii) 6 h post-SAH, iv) 12 h post-SAH, v) 24 h post-SAH and vi) 72 h post-SAH. WB was used to assess changes in the protein expression levels of endogenous ASK1 and p-ASK1. A total of 4 additional rats were divided into sham (n=2) and SAH 24 h (n=2) groups and IF staining was used to evaluate the co-localization of ASK1.

Therapeutic effects of ASK1 inhibitor NQDI-1 on short- and long-term neurological function following SAH. A total of 30 rats were divided into 5 groups (n=6/group) as follows: i) Sham, ii) SAH + vehicle, iii) SAH + 1.0 μg/kg NQDI-1, iv) SAH + 3.0 μg/kg NQDI-1 and v) SAH + 10.0 μg/kg NQDI-1. The modified Garcia and beam balance scores were used to assess short-term neurological function 24 h following SAH. Based on the extent of the short-term neurological improvement, 3.0 μg/kg NQDI-1 was assessed to be the most appropriate dose group and this dose of NQDI-1 was used in subsequent experiments. A total of 30 rats were divided into 3 groups (n=10) as follows: i) Sham, ii) SAH + vehicle and iii) SAH + NQDI-1. A rotarod experiment was used to assess long-term neurological function on days 7, 14 and 21 after SAH, and the Morris water maze test was performed at week 4 after SAH to assess long-term neurological function.

Therapeutic effects of ASK1 inhibitor NQDI-1 on oxidative stress and apoptosis. A total of 12 rats were divided into 3 groups (n=4/group) as follows: i) Sham, ii) SAH + vehicle and iii) SAH + NQDI-1. (DHE) staining was performed to assess oxidative stress and TUNEL staining was used to assess neuronal apoptosis 24 h after SAH.

Role of ASK1/p38 and JNK signaling pathway in the therapeutic effects of NQDI-1. A total of 48 rats were divided into 8 groups (n=6/group) as follows: i) Sham, ii) SAH, iii) SAH + vehicle, iv) SAH + NQDI-1, v) SAH + scrambled (Scr) short interfering (si)RNA, vi) SAH + ASK1 siRNA, vii) SAH + BMS-582949 and viii) SAH + SP600125 groups. The ASK1 siRNA, the p38 inhibitor BMS-582949 or the JNK inhibitor SP600125 were injected to assess whether ASK1, p38 and JNK were involved in the neuroprotective effects of NQDI-1.

Statistical analysis. The data were presented as the mean ± standard deviation and the experimental data of WB were obtained in 6 independent replicates, while DHE staining and TUNEL staining were performed as 4 independent replicates. Data were analyzed using SPSS version 17 (SPSS, Inc.). Data from the Morris water maze test were assessed using a mixed ANOVA/two-way repeated measures ANOVA, followed by the LSD post hoc test. Data from the remaining experiments were tested for normal distribution using the Shapiro-Wilk normal distribution test followed by one-way ANOVA followed by Tukey's post hoc multiple comparison test. Graphs were plotted using GraphPad Prism 7 (GraphPad Software, Inc.). $P<0.05$ was considered to indicate a statistically significant difference.

Results

Mortality and SAH severity. A total of 191 SD rats were used in the present study, of which 8 rats were excluded due to only mild SAH (SAH grading score ≤8). Of the SD rats used in the experiments, 34 rats were in the sham group and 149 rats underwent SAH modeling. No rats in the sham group died; however, 23 rats died following SAH modeling (mortality rate 15.4%) (Tables SI-V). Compared with the sham group, clots in the subarachnoid space were primarily located near the Willis ring and on both sides of the basilar artery following SAH modeling (Fig. 1A). The SAH grading score 24 h post-SAH modeling demonstrated no significant difference in the severity of hemorrhage between all non-sham groups, and a significant difference between sham and all non-sham groups (Fig. 1B).

Protein expression changes and cellular localization of ASK1 following SAH. The protein expression levels of ASK1 increased and reached a peak at 24 h in the brain following SAH (Fig. 1C and D). However, the ratio of the protein expression of p-ASK1/ASK1 demonstrated no significant difference (Fig. 1C and E). Cellular localization of ASK1 with NeuN-positive neurons, Iba-1-positive microglia and GFAP-positive astrocytes was demonstrated in both the sham and SAH 24 h group (Fig. 1F-H).

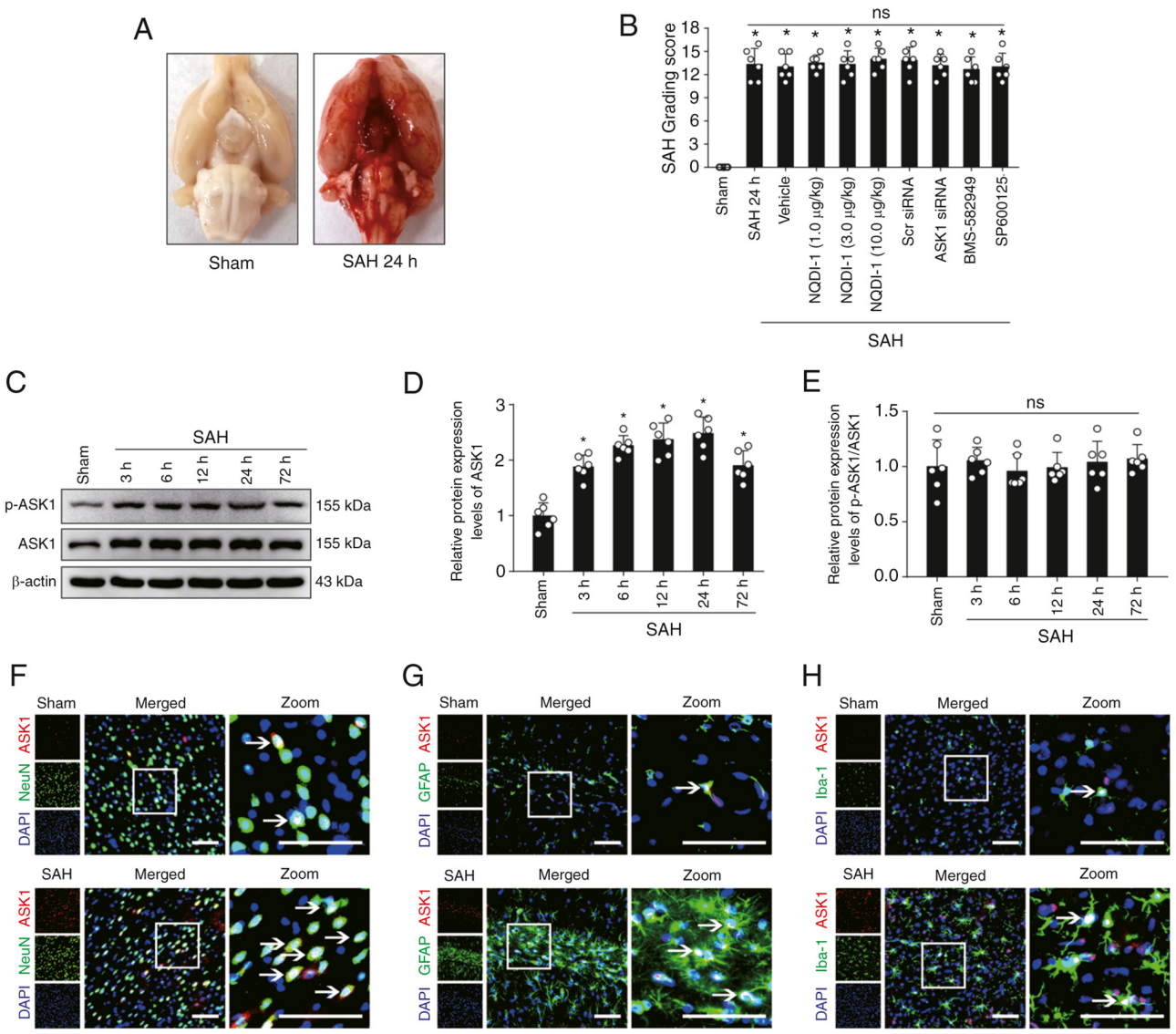

Figure 1. Expression changes and cellular localization of ASK1 in rat brain tissue following SAH. (A) Representative images of rat brain tissue in the sham and SAH 24 h groups. (B) SAH score of rats 24 h after SAH modeling (n=6; Scr siRNA was used as the siRNA control). (C) Western blotting images and semi-quantitative analysis of (D) ASK1 and (E) p-ASK1/ASK1 protein expression levels (n=6). Immunofluorescence of ASK1 with (F) NeuN-positive neurons, (G) Iba-1-positive microglia and (H) GFAP-positive astrocytes. White boxes indicate the location of the zoom plots and white arrows indicate that ASK1 co-localizes with neuronal cells. Scale bar, 50 μm. All data are presented as mean ± standard deviation. *P<0.05 vs. sham. ASK1, apoptosis signal-regulating kinase 1; SAH, subarachnoid hemorrhage; Scr, scrambled; siRNA, small interfering RNA; NQDI-1, ethyl-2,7-dioxo-2,7-dihydro-3H-naphtho(1,2,3-de)quinoline-1-carboxylate; GFAP, glial fibrillary acidic protein; ns, not significant.

ASK1 inhibitor NQDI-1 improves short-term neurological functions 24 h after SAH. NQDI-1 (1, 3 and 10 μg/kg) was injected intracerebroventricularly 1 h after SAH. Rats undergoing SAH modeling had significantly lower modified Garcia and beam balance scores 24 h after SAH modeling; however, all three doses of NQDI-1 led to a significant partial improvement in short-term neurological function (Fig. 2A and B). The modified Garcia scores were significantly higher in the SAH + NQDI-1 (3.0 μg/kg) group compared with the SAH + NQDI-1 (1.0 μg/kg) group; however, no statistically significant differences were demonstrated compared with the SAH + NQDI-1 (10.0 μg/kg) group (Fig. 2A and B), which suggested that further increasing the concentration of NQDI-1 did not elicit further improvement in short-term neurological function following SAH. Therefore, NQDI-1 (3.0 μg/kg) was considered to be the effective optimal concentration and was used in subsequent experiments.

ASK1 inhibitor NQDI-1 improves long-term neurological functions after SAH. Using starting speeds of 5 or 10 rpm for the Rotarod test, fall latency was significantly decreased in the SAH + vehicle group compared with the sham group, whereas the fall latency was significantly prolonged following intracerebroventricular injection of NQDI-1 compared with the SAH + vehicle group (Fig. 2C and D). Furthermore, during days 1-5 of the training phase of the Morris water maze test at week 4 post-SAH, the SAH + vehicle group demonstrated significantly longer escape latency and swimming distance compared with the sham group, whereas NQDI-1 treatment demonstrated a significant decrease compared with the SAH + vehicle group (Fig. 2E-G). On the testing phase with removal of the underwater circular platform, no significant differences were observed in swimming velocity between the three groups (Fig. 2H). The probe quadrant duration was significantly

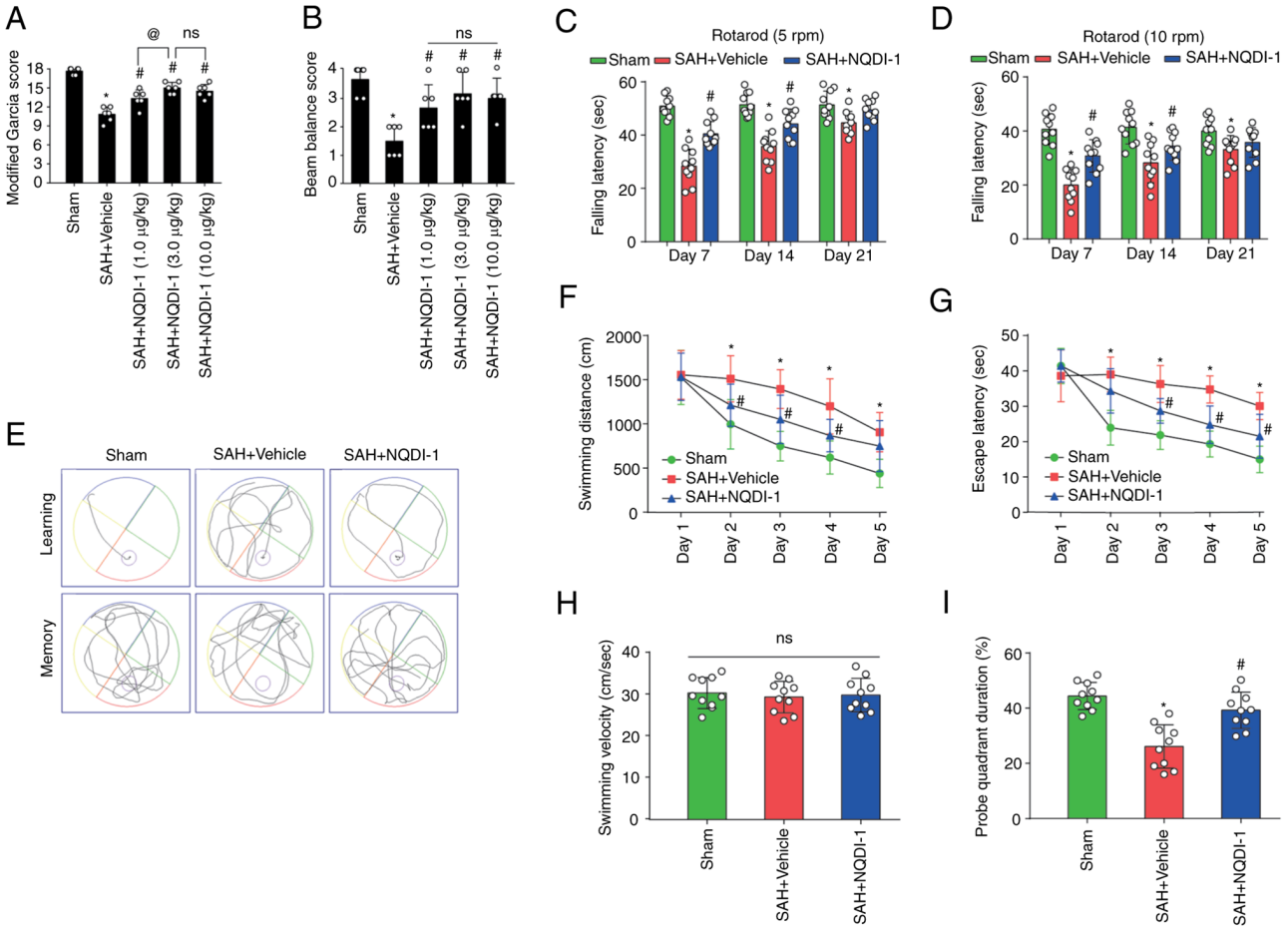

Figure 2. ASK1 inhibitor NQDI-1 improves short- and long-term neurological function following SAH. The therapeutic effects of NQDI-1 on the (A) modified Garcia score and (B) beam balance score 24 h post-SAH in rats (n=6). Fall latency of rats in the Rotarod test at initial speeds of (C) 5 and (D) 10 rpm on days 7, 14 and 21 after SAH (n=10). (E) Representative images of the swimming trajectory in the Morris water maze test. (F) Swimming distances and (G) escape latency training phase from day 1 to day 5 of the Morris water maze test during week 4 after SAH (n=10). (H) Mean swimming velocity and (I) probe duration in the target quadrant during the testing phase of the Morris water maze test during week 4 post-SAH (n=10) Data are presented as the mean ± standard deviation. *P<0.05 vs. sham; #P<0.05 vs. SAH + vehicle; @P<0.05 vs. SAH + NQDI-1 (1.0 μg/kg). ASK1, apoptosis signal-regulating kinase 1; SAH, subarachnoid hemorrhage; NQDI-1, ethyl-2,7-dioxo-2,7-dihydro-3H-naphtho(1,2,3_de)quinoline-1-carboxylate; GFAP, glial fibrillary acidic protein; ns, not significant; rpm, revolutions per minute.

shorter in the SAH + vehicle group compared with the sham group and NQDI-1 treatment significantly prolonged the exploration time compared with the SAH + vehicle group (Fig. 2I).

ASK1 inhibitor NQDI-1 decreases oxidative stress and neuronal apoptosis 24 h post-SAH. The level of oxidative stress was measured using DHE staining and the proportion of apoptotic neurons was assessed using the percentage of TUNEL-positive neurons 24 h after SAH. The percentage of DHE-positive cells was significantly higher in the SAH + vehicle group compared with the sham group and NQDI-1 treatment significantly decreased this compared with the SAH + vehicle group (Fig. 3A and C). The percentage of TUNEL-positive neurons was significantly higher in the SAH + vehicle group compared with the sham group. However, the percentage of TUNEL-positive neurons decreased significantly following treatment with NQDI-1 compared with the SAH + vehicle group (Fig. 3B and D).

ASK1 siRNA, BMS-582949 and SP600125 improve short-term neurological functions 24 h post-SAH. Compared with the SAH + Scr siRNA group or SAH + vehicle group, administration of ASK1 siRNA, BMS-582949 or SP600125 demonstrated significant improvement in the modified Garcia and beam balance score (Fig. 4A and B).

NQDI-1 attenuates oxidative stress and apoptosis after SAH via decreased phosphorylation of ASK1, p38 and JNK. The protein expression levels of ASK1, p-p38, p-JNK, 4-HNE, HO-1, Bax and Bcl-2 were significantly higher after SAH compared with the sham group; however, the ratio of p-ASK1/ASK1 was not significantly different (Fig. 5A-M). The injection of vehicle or Scr siRNA did not induce significant differences in the protein expression levels compared with the SAH group. Compared with the SAH + vehicle group, treatment using NQDI-1 caused a significant decrease in the protein expression levels of p-ASK1/ASK1, p-p38, p-JNK, 4-HNE and Bax, whereas protein expression levels of HO-1 and Bcl-2 were significantly increased. Compared with the SAH + Scr siRNA group, protein expression levels of ASK1 significantly decreased following injection of ASK1 siRNA. Treatment with ASK1 siRNA also resulted in a significant decrease in the protein expression levels of

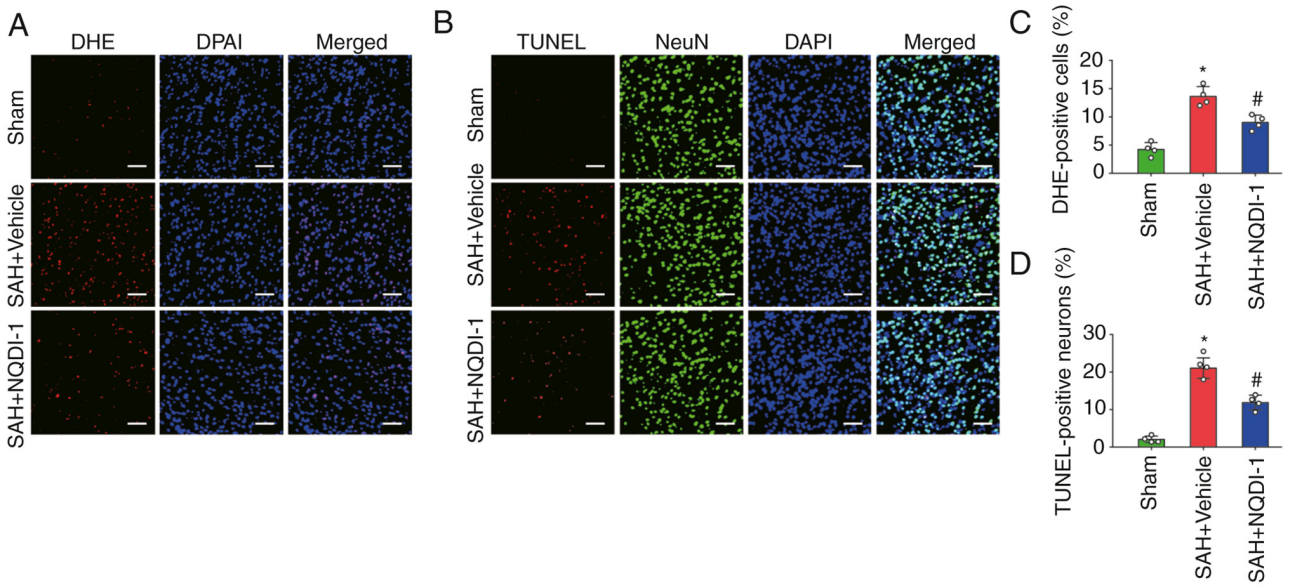

Figure 3. ASK1 inhibitor NQDI-1 decreases oxidative stress and neuronal apoptosis 24 h after SAH. (A) Photomicrographs of DHE staining. Scale bar, 50 μm. (B) Photomicrographs of TUNEL staining. Scale bar, 50 μm. (C) Quantitative analysis of DHE staining (n=4). (D) Quantitative analysis of TUNEL staining (n=4). All data are presented as the mean ± standard deviation. *P<0.05 vs. sham; $^{\#}$P<0.05 vs. SAH + vehicle. ASK1, apoptosis signal-regulating kinase 1; SAH, subarachnoid hemorrhage; NQDI-1, ethyl-2,7-dioxo-2,7-dihydro-3H-naphtho(1,2,3-de)quinoline-1-carboxylate; DHE, dihydroethidium.

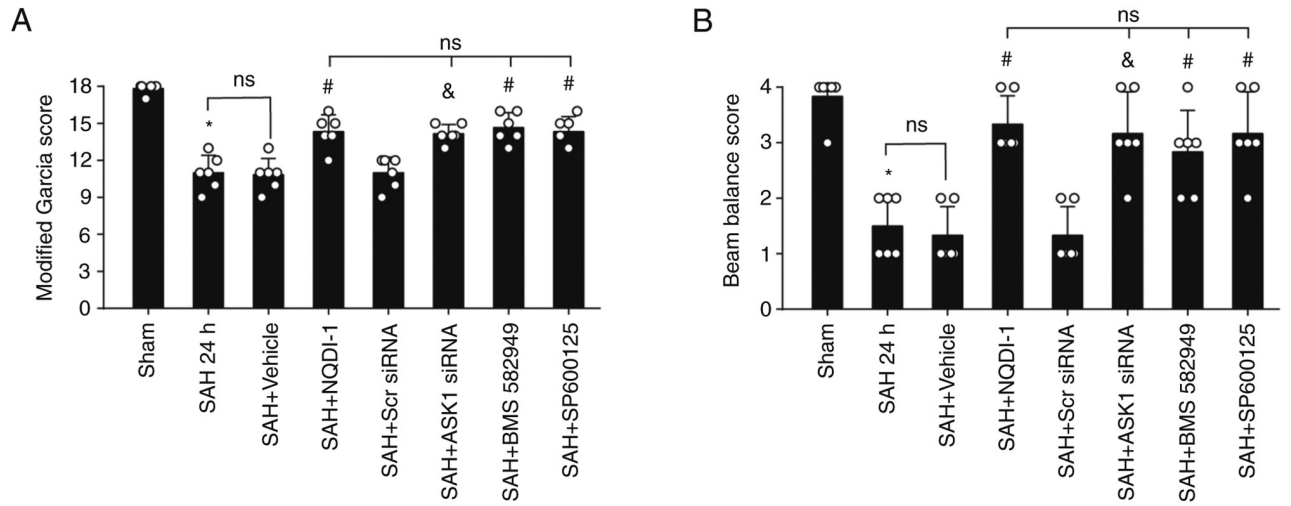

Figure 4. ASK1 siRNA, p38 inhibitor BMS 582949 and JNK inhibitor SP600125 improve short-term neurological function 24 h post-SAH. (A) Modified Garcia score and (B) beam balance score 24 h post-SAH in rats (n=6). Scr siRNA was used as the control. All data are presented as the mean ± standard deviation. *P<0.05 vs. sham; $^{\#}$P<0.05 vs. SAH + vehicle; $^{\&}$P<0.05 vs. SAH + Scr siRNA. ns, not significant; ASK1, apoptosis signal-regulating kinase 1; SAH, subarachnoid hemorrhage; Scr, scrambled; siRNA, small interfering RNA.

p-p38, p-JNK, 4-HNE and Bax and a significant increase in HO-1 and Bcl-2 expression compared with the SAH + Scr siRNA group.

p38 inhibitor BMS-582949 reduces the protein expression levels of p-p38 but has no effect on p-ASK1, ASK1 or p-JNK protein expression levels. Treatment with the p38 inhibitor BMS-582949 demonstrated a significant decrease in protein expression levels of p-p38, 4-HNE and Bax and also significantly increased protein expression of HO-1 and Bcl-2 compared with the SAH + vehicle group; however, the protein expression levels of ASK1, p-ASK1/ASK1 and p-JNK demonstrated no significant differences (Fig. 6A-M).

JNK inhibitor SP600125 decreases protein expression level of p-JNK but has no effect on p-ASK1, ASK1 or p-p38 protein expression levels. Treatment with JNK inhibitor SP600125 caused a significant decrease in the protein expression levels of p-JNK, 4-HNE and Bax and a significant increase in HO-1 and Bcl-2 protein expression levels compared with the SAH + vehicle group; however, protein expression levels of ASK1, p-ASK1/ASK1 and p-p38 were not significantly altered (Fig. 7A-M).

Discussion

In the present study, protein expression levels of ASK1 and p-ASK1 were elevated following SAH. ASK1 inhibitor NQDI-1

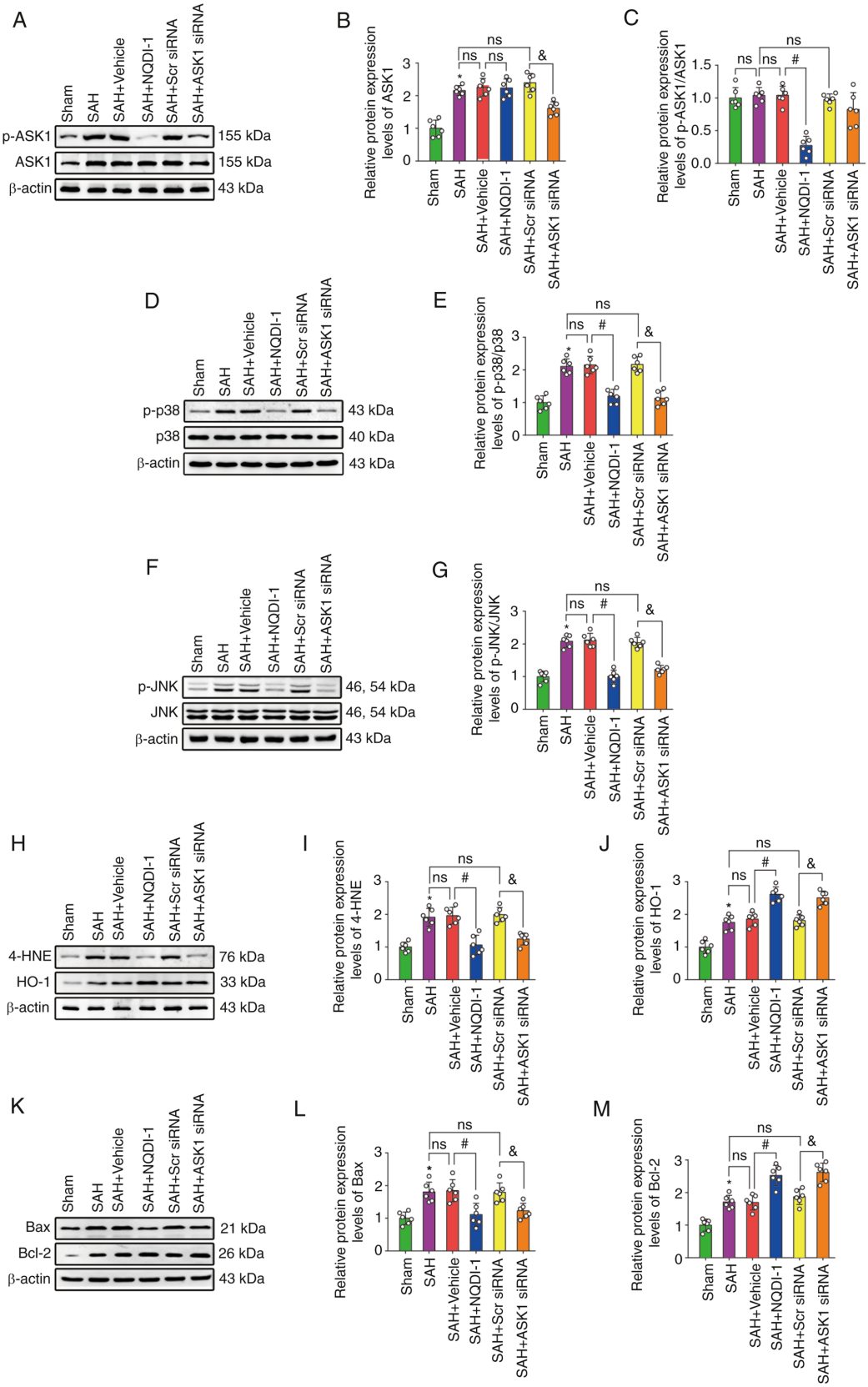

Figure 5. NQDI-1 attenuates oxidative stress and apoptosis following SAH via decreased phosphorylation of ASK1, p38 and JNK. (A) Western blotting images of p-ASK1 and ASK1. Semi-quantitative analysis of (B) ASK1 protein expression levels (n=6) and (C) p-ASK1/ASK1 protein expression levels (n=6). (D) Western blotting images of p-p38 and p38. (E) Semi-quantitative analysis of p-p38/p38 protein expression levels (n=6). (F) Western blotting images of p-JNK and JNK. (G) Semi-quantitative analysis of p-JNK/JNK protein expression levels (n=6). (H) Western blotting images of 4-HNE and HO-1. Semi-quantitative analysis of (I) 4-HNE protein expression levels (n=6) and (J) HO-1 protein expression levels (n=6). (K) Western blotting images of Bax and Bcl-2. Semi-quantitative analysis of (L) Bax protein expression levels (n=6) and (M) Bcl-2 protein expression levels (n=6). Scr siRNA was used as the control. All data are presented as the mean ± standard deviation. *P<0.05 vs. sham; $^{\#}$P<0.05 vs. SAH + vehicle; $^{\&}$P<0.05 vs. SAH + Scr siRNA. ASK1, apoptosis signal-regulating kinase 1; SAH, subarachnoid hemorrhage; NQDI-1, ethyl-2,7-dioxo-2,7-dihydro-3H-naphtho(1,2,3-de)quinoline-1-carboxylate; p, phosphorylated; 4-HNE, 4 hydroxynonenal; HO-1, heme oxygenase 1; Scr, scrambled; siRNA, small interfering RNA.

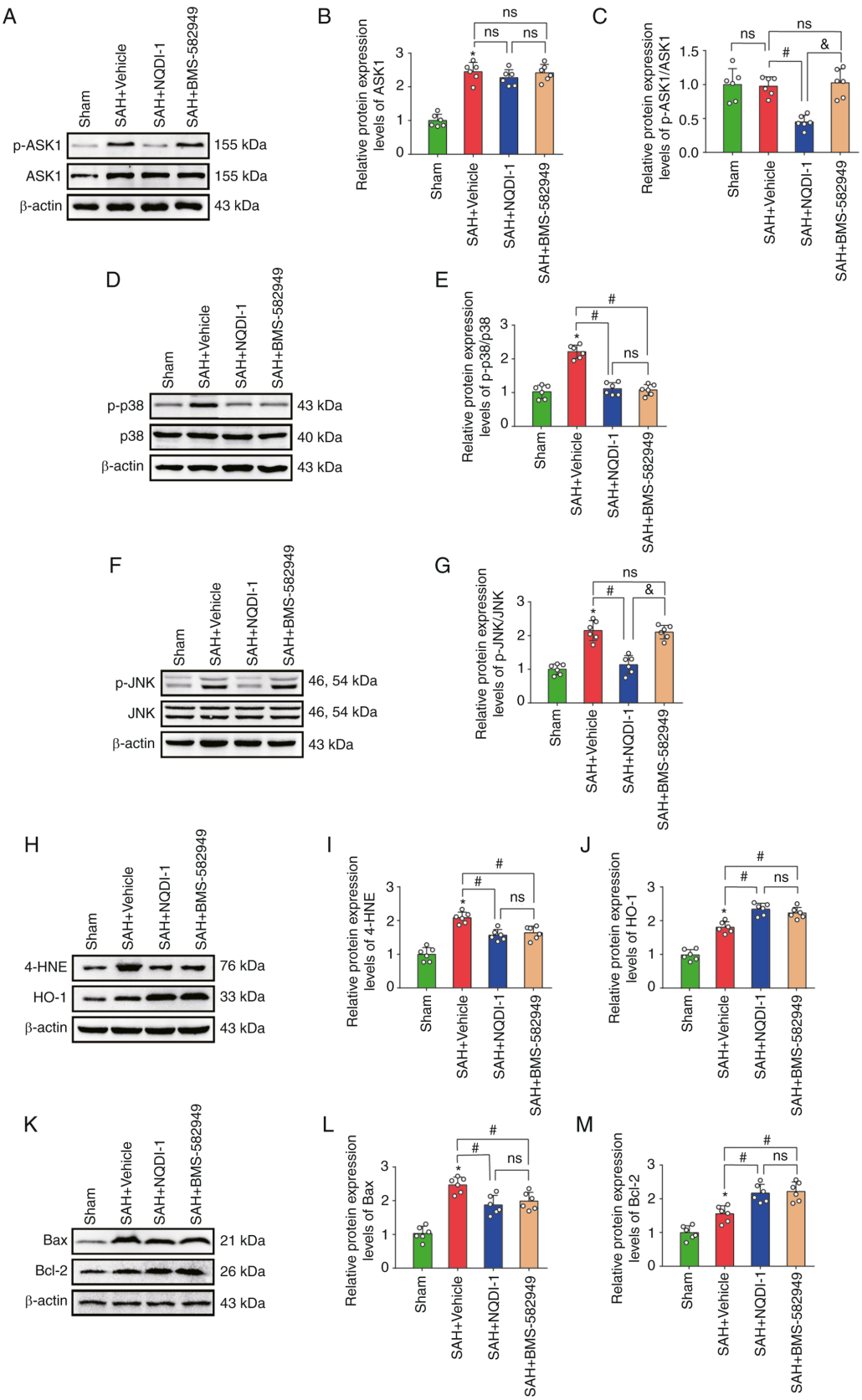

Figure 6. p38 inhibitor BMS 582949 decreases protein expression of p-p38 but has no effect on protein expression levels of p-ASK1, ASK1 or p-JNK. (A) Western blotting images of p-ASK1 and ASK1. Semi-quantitative analysis of (B) ASK1 protein expression levels (n=6) and (C) p-ASK1/ASK1 protein expression levels (n=6). (D) Western blotting images of p-p38 and p38. (E) Semi-quantitative analysis of p-p38/p38 protein expression levels (n=6). (F) Western blotting images of p-JNK and JNK. (G) Semi-quantitative analysis of p-JNK/JNK protein expression levels (n=6). (H) Western blotting images of 4-HNE and HO-1. Semi-quantitative analysis of (I) 4-HNE protein expression levels (n=6) and (J) HO-1 protein expression levels (n=6). (K) Western blotting images of Bax and Bcl-2. Semi-quantitative analysis of (L) Bax protein expression levels (n=6) and (M) Bcl-2 protein expression levels (n=6). Data are presented as the mean ± standard deviation. *P<0.05 vs. sham; #P<0.05 vs. SAH + vehicle; &P<0.05 vs. SAH + NQDI-1, apoptosis signal-regulating kinase 1; SAH, subarachnoid hemorrhage; NQDI-1, ethyl-2,7-dioxo-2,7-dihydro-3H-naphtho(1,2,3-de)quinoline-1-carboxylate; p, phosphorylated; 4-HNE, 4 hydroxynonenal; HO-1, heme oxygenase 1; Scr, scrambled; siRNA, small interfering RNA; ns, not significant.

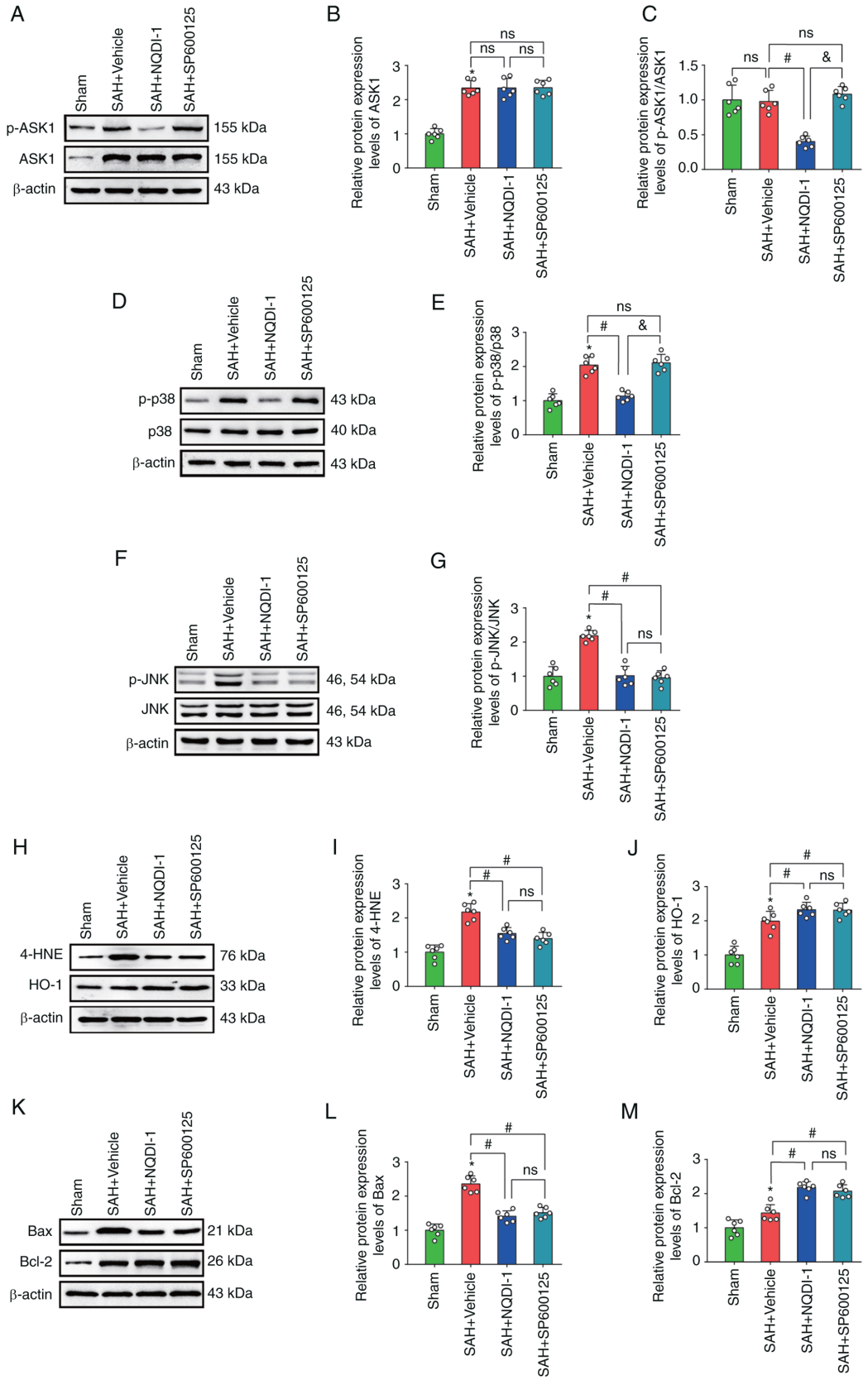

Figure 7. JNK inhibitor SP600125 decreases expression of p-JNK, but has no effect on p-ASK1, ASK1 or p-p38. (A) Western blotting images of p-ASK1 and ASK1. Semi-quantitative analysis of (B) ASK1 protein expression levels (n=6) and (C) p-ASK1/ASK1 protein expression levels (n=6). (D) Western blotting images of p-p38 and p38. (E) Semi-quantitative analysis of p-p38/p38 protein expression levels (n=6). (F) Western blotting images of p-JNK and JNK. (G) Semi-quantitative analysis of p-JNK/JNK protein expression levels (n=6). (H) Western blotting images of 4-HNE and HO-1. Semi-quantitative analysis of (I) 4-HNE protein expression levels (n=6) and (J) HO-1 protein expression levels (n=6). (K) Western blotting images of Bax and Bcl-2. Semi-quantitative analysis of (L) Bax protein expression levels (n=6) and (M) Semi Bcl-2 protein expression levels (n=6). All data are presented as mean ± standard deviation. *P<0.05 vs. sham; #P<0.05 vs. SAH + vehicle; &P<0.05 vs. SAH + NQDI-1, apoptosis signal-regulating kinase 1; SAH, subarachnoid hemorrhage; NQDI-1, ethyl-2,7-dioxo-2,7-dihydro-3H-naphtho(1,2,3-de)quinoline-1-carboxylate; p, phosphorylated; 4-HNE, 4 hydroxynonenal; HO-1, heme oxygenase 1; Scr, scrambled; siRNA, small interfering RNA; ns, not significant.

improved short- and long-term neurological function after SAH and decreased oxidative stress and neuronal apoptosis via inhibition of ASK1 phosphorylation and the ASK1/p38 and JNK signaling pathway in EBI following SAH.

ASK1 is a member of the MAP3K family and its activation in response to numerous types of cellular stress mediates different types of cellular damage (31). For certain diseases involving oxidative stress and apoptosis, decreased protein expression of ASK1 or inhibition of its phosphorylation may have a beneficial role by decreasing oxidative stress and apoptosis (32). To the best of our knowledge, however, the role and underlying mechanism of action of ASK1 and its inhibitor NQDI-1 have not previously been reported in SAH. The present study demonstrated that the protein expression levels of ASK1 and p-ASK1 were significantly increased following SAH modeling, which suggested that ASK1 may serve a role in EBI after SAH. Furthermore, ASK1 was co-expressed in neurons, microglia and astrocytes, which suggested a wide role for ASK1 in a variety of neuronal cells following SAH.

NQDI-1 is a specific inhibitor of ASK1 and its functional role has been previously demonstrated using *in vitro* kinase assays (11,33). In a mouse model of acute pancreatitis, NQDI-1 decreases pancreatic follicular cell necrosis through decrease of ROS production and receptor interacting serine/threonine kinase 3 and p-mixed lineage kinase domain-like pseudokinase protein expression levels (34). In ischemic brain injury, NQDI-1 inhibition of ASK1 decreases matrix metalloproteinase 9 activity and subsequent neuronal apoptosis in brain endothelial cells (35). In the present study, different concentrations of NQDI-1 were injected intracerebroventricularly, which significantly improved the modified Garcia and balance beam test score, which suggested that NQDI-1 led to improvements in short-term neurological function following SAH.

For long-term neurological function, two methods were used to assess function over different time periods (36). The Rotarod test was used to assess the coordinated balance of locomotion on day 7, 14 and 21. At initial speeds of 5 or 10 rpm, the fall latency of rats in the SAH + vehicle group was significantly shorter compared with that in the sham group and treatment with NQDI-1 led to a significant increase. The Morris water maze test was used to assess the spatial memory and learning ability of rats during the fourth week. During the training phase of days 1-5, the SAH group rats swam for significantly longer times and for further distances compared with the sham group and NQDI-1 treatment decreased this phenomenon. During the testing phase, no significant differences were demonstrated in the swimming speed between groups of rats. After removal of the platform, the time spent exploring the target quadrant was observed and counted for each group of rats. Following SAH, rats searched for the target quadrant for a shorter time, which indicated that SAH modeling led to more ambiguous spatial localization and memory in rats and impaired long-term memory capacity, whereas NQDI-1 treatment demonstrated improvements in these outcomes. Rotarod experiment and the Morris water maze test results suggested that NQDI-1 improved long-term neurological function after SAH.

Oxidative stress and neuroapoptosis are key pathological changes of EBI following SAH (37). In steady-state cells, ROS are primarily byproducts of respiration produced by the mitochondrial electron respiratory chain and moderate levels of ROS repair damaged DNA and serve a physiological role in the promotion of cell survival (38). Upon SAH, due to the autoxidation of blood in the subarachnoid space, ROS catalysis by heme and intracellular mitochondrial dysfunction, electrons escape into the cytoplasm and the antioxidant system is insufficient to compensate, which results in accumulation of large amounts of ROS in neuronal cells (39), which leads to oxidative stress damage. Therefore, therapeutic strategies that target oxidative stress and apoptosis may be considered effective therapeutic directions following SAH. In the present study, ROS and oxidative stress of brain tissues were assessed using DHE, which is oxidized into ethidium and produces a red fluorescent signal (40). The percentage of DHE-positive cells significantly increased in the SAH + vehicle group, whereas a decrease was demonstrated in the percentage of DHE-positive cells in the SAH + NQDI-1 group, which suggested that NQDI-1 decreased oxidative stress. Apoptosis was assessed using TUNEL and the percentage of TUNEL-positive neuronal cells following SAH modeling significantly increased, whereas NQDI-1 significantly decreased the percentage of TUNEL-positive neuronal cells. It may be hypothesized that treatment NQDI-1 decreased oxidative stress and apoptosis in EBI following SAH.

The effect of NQDI-1 on ASK1 and the potential underlying molecular mechanism were evaluated. The effects of NQDI-1 on protein expression levels of ASK1 and p-ASK1 were first assessed. The ratio of p-ASK1/ASK1 did not change following SAH, which suggested that changes in the phosphorylation of ASK1 were similar to those of ASK1 protein expression levels. Treatment with NQDI-1 demonstrated a significant decrease in p-ASK1 protein expression levels but demonstrated no effect on ASK1 compared with the SAH + vehicle group, which suggested that NQDI-1 exerted its neuroprotective effects primarily via inhibition of ASK1 phosphorylation. Subsequently, protein expression levels of both p-ASK1 and ASK1 were knocked down using ASK1 siRNA, following which protein expression levels of p-p38 and p-JNK were significantly decreased, which suggested that ASK1 was activated primarily via phosphorylation.

The p38, MAPK and JNK signaling pathways are widely expressed in brain tissue (41). Activated p38, MAPK and JNK enhance tumor necrosis factor-induced apoptosis, participate in the Fas/FasL system, phosphorylate P53 and induce mitochondrial translocation of BAX and other pathways to promote apoptosis (42). Inhibition of the phosphorylation activation of p38 MAPK and JNK decreases oxidative stress and neuronal apoptosis, alleviates EBI and improves the prognosis of the SAH rat model (43). After injection of the p38 inhibitor BMS-582949, the WB results demonstrated that it significantly inhibited phosphorylation of p38 and significantly downregulated expression levels of oxidative stress and apoptosis-associated proteins. However, BMS-582949 did not cause a significant difference in the protein expression levels of p-ASK1, ASK1 or p-JNK. Similarly, the JNK inhibitor SP600125 significantly inhibited phosphorylation of JNK, but demonstrated no significant effect on p-ASK1, ASK1 or p-p38 protein expression levels. These results suggested that p38 and JNK were downstream of p-ASK1 and that ASK1 caused oxidative stress and

apoptosis following SAH via phosphorylation-activated p38 and JNK.

There were certain limitations associated with the present study. Firstly, NQDI-1 was only administered once via intracerebroventricular injection 1 h after SAH; therefore, the current study was not suitable to determine the optimal therapeutic window for NQDI-1 treatment and future studies are required to address this issue. Secondly, the present study was a pilot study to evaluate the effect of inhibition of ASK1 on neurological function and to explore whether NQDI-1 had a therapeutic effect following SAH. The role of ASK1 in astrocytes or microglia and the pharmacokinetics of NQDI-1 require further elucidation in future studies. The Morris water maze test was only performed during the fourth week post-SAH; therefore, potential changes in early ability of spatial memory and learning ability may not have been assessed. Finally, IF was used to assess ASK1 co-localization; however, only 2 animals/experimental group was assessed. The small sample size is a limitation of the present study that may result in inappropriate conclusions and should only be used for qualitative, rather than quantitative, assessment.

In conclusion, ASK1 inhibitor NQDI-1 decreased oxidative stress and apoptosis and improved short and long-term neurological function following SAH via inhibition of ASK1 phosphorylation and the p38 and JNK signaling pathways. NQDI-1 may be a potential therapeutic agent for treatment of SAH.

Acknowledgements

Not applicable.

Funding

The present study was supported by The National Natural Science Foundation of China (grant no. 81870944), The Beijing Science and Technology Plan Subject: Beijing-Tianjin-Hebei Collaborative Innovation Promotion Project (grant no. Z181100009618035), The National Natural Science Foundation of China (grant no. 81771233), Beijing Municipal Administration of Hospitals' Ascent Plan (grant no. DFL20190501) and Research and Promotion Program of Appropriate Techniques for Intervention of Chinese High-risk Stroke People (grant no. GN-2020R0007).

Availability of data and materials

The datasets used and/or analyzed during the current study are available from the corresponding author on reasonable request.

Authors' contributions

JD, WY, JJ, FL and AL participated in the experimental design. JD, JJ, JW and XY performed the experiments and collected and analyzed the data. XY, FL and AL interpreted the data. JD and WY drafted the manuscript. XY, FL and AL revised the manuscript and proofread the language. All authors have read and approved the final manuscript. JD, JW and FL confirm the authenticity of all the raw data.

Ethics approval and consent to participate

All experimental procedures were approved by the Institutional Animal Care and Use Committee of Central South University (approval. no. 2019sydw0104).

Patient consent for publication

Not applicable.

Competing interests

The authors declare that they have no competing interests.

References

1. Lawton MT and Vates GE: Subarachnoid Hemorrhage. N Engl J Med 377: 257-266, 2017.
2. GBD 2019 Stroke Collaborators: Global, regional, and national burden of stroke and its risk factors, 1990-2019: A systematic analysis for the Global Burden of Disease Study 2019. Lancet Neurol 20: 795-820, 2021.
3. Osgood ML: Aneurysmal subarachnoid hemorrhage: Review of the pathophysiology and management strategies. Curr Neurol Neurosci Rep 21: 50, 2021.
4. Topkoru B, Egemen E, Solaroglu I and Zhang JH: Early brain injury or vasospasm? An overview of common mechanisms. Curr Drug Targets 18: 1424-1429, 2017.
5. Merlini E, Coleman MP and Loreto A: Mitochondrial dysfunction as a trigger of programmed axon death. Trends Neurosci 45: 53-63, 2022.
6. Kowalczyk P, Sulejczak D, Kleczkowska P, Bukowska-Ośko I, Kucia M, Popiel M, Wietrak E, Kramkowski K, Wrzosek K and Kaczyńska K: Mitochondrial oxidative stress-A causative factor and therapeutic target in many diseases. Int J Mol Sci 22: 13384, 2021.
7. Matsushita M, Nakamura T, Moriizumi H, Miki H and Takekawa M: Stress-responsive MTK1 SAPKKK serves as a redox sensor that mediates delayed and sustained activation of SAPKs by oxidative stress. Sci Adv 6: eaay9778, 2020.
8. Gao Y, Yan Y, Fang Q, Zhang N, Kumar G, Zhang J, Song LJ, Yu J, Zhao L, Zhang HT and Ma CG: The Rho kinase inhibitor fasudil attenuates $A\beta_{1-42}$-induced apoptosis via the ASK1/JNK signal pathway in primary cultures of hippocampal neurons. Metab Brain Dis 34: 1787-1801, 2019.
9. Volynets GP, Chekanov MO, Synyugin AR, Golub AG, Kukharenko OP, Bdzhola VG and Yarmoluk SM: Identification of 3H-naphtho[1,2,3-de]quinoline-2,7-diones as inhibitors of apoptosis signal-regulating kinase 1 (ASK1). J Med Chem 54: 2680-2686, 2011.
10. Zhang QS, Kurpad DS, Mahoney MG, Steinbeck MJ and Freeman TA: Inhibition of apoptosis signal-regulating kinase 1 alters the wound epidermis and enhances auricular cartilage regeneration. PLoS One 12: e0185803, 2017.
11. Hao H, Li S, Tang H, Liu B, Cai Y, Shi C and Xiao X: NQDI-1, an inhibitor of ASK1 attenuates acute perinatal hypoxic-ischemic cerebral injury by modulating cell death. Mol Med Rep 13: 4585-4592, 2016.
12. Chen S, Zuo Y, Huang L, Sherchan P, Zhang J, Yu Z, Peng J, Zhang J, Zhao L, Doycheva D, *et al*: The MC receptor agonist RO27-3225 inhibits NLRP1-dependent neuronal pyroptosis via the ASK1/JNK/p38 MAPK pathway in a mouse model of intracerebral haemorrhage. Br J Pharmacol 176: 1341-1356, 2019.
13. Du X, Liu H, Liu X, Chen X, Yuan L, Ma Y, Huang H, Wang Y, Wang R, Zhang S, *et al*: Microcystin-LR induces ovarian injury and apoptosis in mice via activating apoptosis signal-regulating kinase 1-mediated P38/JNK pathway. Ecotoxicol Environ Saf 213: 112066, 2021.
14. Chang CY, Li JR, Wu CC, Wang JD, Liao SL, Chen WY, Wang WY and Chen CJ: Endoplasmic reticulum stress contributes to indomethacin-induced glioma apoptosis. Int J Mol Sci 21: 557, 2020.
15. Win S, Than TA, Zhang J, Oo C, Min RWM and Kaplowitz N: New insights into the role and mechanism of c-Jun-N-terminal kinase signaling in the pathobiology of liver diseases. Hepatology 67: 2013-2024, 2018.

16. Percie du Sert N, Ahluwalia A, Alam S, Avey MT, Baker M, Browne WJ, Clark A, Cuthill IC, Dirnagl U, Emerson M, *et al*: Reporting animal research: Explanation and elaboration for the ARRIVE guidelines 2.0. PLoS Biol 18: e3000411, 2020.
17. McPherson C: Regulation of animal care and research? NIH's opinion. J Anim Sci 51: 492-496, 1980.
18. Boivin GP, Hickman DL, Creamer-Hente MA, Pritchett-Corning KR and Bratcher NA: Review of CO_2 as a euthanasia agent for laboratory rats and mice. J Am Assoc Lab Anim Sci 56: 491-499, 2017.
19. Luo K, Wang Z, Zhuang K, Yuan S, Liu F and Liu A: Suberoylanilide hydroxamic acid suppresses axonal damage and neurological dysfunction after subarachnoid hemorrhage via the HDAC1/HSP70/TDP-43 axis. Exp Mol Med 54: 1423-1433, 2022.
20. Xie Z, Enkhjargal B, Nathanael M, Wu L, Zhu Q, Zhang T, Tang J and Zhang JH: viaExendin-4 preserves blood-brain barrier integrity glucagon-like peptide 1 receptor/activated protein kinase-dependent nuclear Factor-Kappa B/Matrix Metalloproteinase-9 inhibition after subarachnoid hemorrhage in rat. Front Mol Neurosci 14: 750726, 2021.
21. Craft TK and DeVries AC: Role of IL-1 in poststroke depressive-like behavior in mice. Biol Psychiatry 60: 812-818, 2006.
22. Xie Z, Enkhjargal B, Wu L, Zhou K, Sun C, Hu X, Gospodarev V, Tang J, You C and Zhang JH: Exendin-4 attenuates neuronal death via GLP-1R/PI3K/Akt pathway in early brain injury after subarachnoid hemorrhage in rats. Neuropharmacology 128: 142-151, 2018.
23. Liu C, Lin J, Wrobleski ST, Lin S, Hynes J, Wu H, Dyckman AJ, Li T, Wityak J, Gillooly KM, *et al*: Discovery of 4-(5-(cyclopropylcarbamoyl)-2-methylphenylamino)-5-methyl-N-propylpyrrolo[1,2-f][1,2,4]triazine-6-carboxamide (BMS-582949), a clinical p38α MAP kinase inhibitor for the treatment of inflammatory diseases. J Med Chem 53: 6629-6639, 2010.
24. Bennett BL, Sasaki DT, Murray BW, O'Leary EC, Sakata ST, Xu W, Leisten JC, Motiwala A, Pierce S, Satoh Y, *et al*: SP600125, an anthrapyrazolone inhibitor of Jun N-terminal kinase. Proc Natl Acad Sci USA 98: 13681-13686, 2001.
25. Dai J, Xu S, Okada T, Liu Y, Zuo G, Tang J, Zhang JH and Shi H: T0901317, an agonist of liver X receptors, attenuates neuronal apoptosis in early brain injury after subarachnoid hemorrhage in rats via liver X receptors/interferon regulatory factor/P53 upregulated modulator of apoptosis/dynamin-1-like protein pathway. Oxid Med Cell Longev 2021: 8849131, 2021.
26. Xiao ZP, Lv T, Hou PP, Manaenko A, Liu Y, Jin Y, Gao L, Jia F, Tian Y, Li P, *et al*: Sirtuin 5-Mediated lysine desuccinylation protects mitochondrial metabolism following subarachnoid hemorrhage in mice. Stroke 52: 4043-4053, 2021.
27. Xu W, Yan J, Ocak U, Lenahan C, Shao A, Tang J, Zhang J and Zhang JH: viaMelanocortin 1 receptor attenuates early brain injury following subarachnoid hemorrhage by controlling mitochondrial metabolism AMPK/SIRT1/PGC-1α pathway in rats. Theranostics 11: 522-539, 2021.
28. Mo J, Enkhjargal B, Travis ZD, Zhou K, Wu P, Zhang G, Zhu Q, Zhang T, Peng J, Xu W, *et al*: AVE 0991 attenuates oxidative stress and neuronal apoptosis via Mas/PKA/CREB/UCP-2 pathway after subarachnoid hemorrhage in rats. Redox Biol 20: 75-86, 2019.
29. He Y, Zheng Z, Liu C, Li W, Zhao L, Nie G and Li H: viaInhibiting DNA methylation alleviates cisplatin-induced hearing loss by decreasing oxidative stress-induced mitochondria-dependent apoptosis the LRP1-PI3K/AKT pathway. Acta Pharm Sin B 12: 1305-1321, 2022.
30. van Lieshout JH, Marbacher S, Muhammad S, Boogaarts HD, Bartels RHMA, Dibué M, Steiger HJ, Hänggi D and Kamp MA: Proposed definition of experimental secondary ischemia for mouse subarachnoid hemorrhage. Transl Stroke Res 11: 1165-1170, 2020.
31. Ogier JM, Nayagam BA and Lockhart PJ: ASK1 inhibition: A therapeutic strategy with multi-system benefits. J Mol Med (Berl) 98: 335-348, 2020.
32. Zhang XS, Lu Y, Li W, Tao T, Peng L, Wang WH, Gao S, Liu C, Zhuang Z, Xia DY, *et al*: Astaxanthin ameliorates oxidative stress and neuronal apoptosis via SIRT1/NRF2/Prx2/ASK1/p38 after traumatic brain injury in mice. Br J Pharmacol 178: 1114-1132, 2021.
33. Chen S, Yu Q, Song Y, Cui Z, Li M, Mei C, Cui H, Cao S and Zhu C: Inhibition of macrophage migration inhibitory factor (MIF) suppresses apoptosis signal-regulating kinase 1 to protect against liver ischemia/reperfusion injury. Front Pharmacol 13: 951906, 2022.
34. Xie X, Yuan C, Yin L, Zhu Q, Ma N, Chen W, Ding Y, Xiao W, Gong W, Lu G, *et al*: NQDI-1 protects against acinar cell necrosis in three experimental mouse models of acute pancreatitis. Biochem Biophys Res Commun 520: 211-217, 2019.
35. Cheon SY, Cho KJ, Kim SY, Kam EH, Lee JE and Koo BN: Blockade of apoptosis signal-regulating kinase 1 attenuates matrix metalloproteinase 9 activity in brain endothelial cells and the subsequent apoptosis in neurons after ischemic injury. Front Cell Neurosci 10: 213, 2016.
36. Zhu Q, Enkhjargal B, Huang L, Zhang T, Sun C, Xie Z, Wu P, Mo J, Tang J, Xie Z and Zhang JH: Aggf1 attenuates neuroinflammation and BBB disruption via PI3K/Akt/NF-κB pathway after subarachnoid hemorrhage in rats. J Neuroinflammation 15: 178, 2018.
37. Wu Y, Liu Y, Zhou C, Wu Y, Sun J, Gao X and Huang Y: Biological effects and mechanisms of caspases in early brain injury after subarachnoid hemorrhage. Oxid Med Cell Longev 2022: 3345637, 2022.
38. Checa J and Aran JM: Reactive oxygen species: Drivers of Physiological and pathological processes. J Inflamm Res 13: 1057-1073, 2020.
39. Zhang Z, Zhang A, Liu Y, Hu X, Fang Y, Wang X, Luo Y, Lenahan C and Chen S: New Mechanisms and Targets of Subarachnoid Hemorrhage: A Focus on Mitochondria. Curr Neuropharmacol 20: 1278-1296, 2022.
40. Liu B, Tian Y, Li Y, Wu P, Zhang Y, Zheng J and Shi H: ACEA Attenuates Oxidative Stress by Promoting Mitophagy via CB1R/Nrf1/PINK1 Pathway after Subarachnoid Hemorrhage in Rats. Oxid Med Cell Longev 2022: 1024279, 2022.
41. Iroegbu JD, Ijomone OK, Femi-Akinlosotu OM and Ijomone OM: ERK/MAPK signalling in the developing brain: Perturbations and consequences. Neurosci Biobehav Rev 131: 792-805, 2021.
42. Anjum J, Mitra S, Das R, Alam R, Mojumder A, Emran TB, Islam F, Rauf A, Hossain MJ, Aljohani ASM, *et al*: A renewed concept on the MAPK signaling pathway in cancers: Polyphenols as a choice of therapeutics. Pharmacol Res 184: 106398, 2022.
43. Wei YX, Zhang DD, Gao YY, Hang CH and Shi JX: Inhibition of the myeloid differentiation primary response protein 88 reducres neuron injury in the early stages of subarachnoid hemorrhage in an in vitro experimental model. J Physiol Pharmacol 73, 2022.

This work is licensed under a Creative Commons Attribution-NonCommercial-NoDerivatives 4.0 International (CC BY-NC-ND 4.0) License.